Luminescent Materials with Spectral Conversion for Renewable Energies:

Photocatalysis and Artificial Photosynthesis

RUBEN ROJAS SIVERIO

Tutor: Dr. Jorge Mendez Ramos

July 9, 2019

Contents

1 Introduction

Since the industrial revolution the emission of greenhouse gases has increased and the concentration of these in the atmosphere reaches the highest level in one million years [1; 2]. This is producing a climate change that could be disastrous to living beings all around the planet because they can not adapt as fast as the weather change.

The greenhouse gases are emitted by the human activity because the main way to obtain energy is based on organic compounds dissociation (more than the 80% of the worldwide total) [3], with the corresponding CO_2 emission. According with the European database [4], this were the areas which produced more CO_2 in 2017:

1. Direct emissions by private households

2. Electricity, gas, steam and air conditioning

3. Constructions and construction works

4. Coke and refined petroleum products

5. Food, beverages and tobacco products

6. Chemicals and chemical products

7. Air transport services

8. Motor vehicles, trailers and semi-trailers

9. Land transport services and transport services via pipelines

10. Machinery and equipment n.e.c.

Most of the things enumerated here are perfectly avoidable by changing the way of obtaining the energy, both for electricity and for transport. If these areas were covered by CO_2-free methods, the greenhouse gases emission would decrease drastically, being possible to fight them more easily.

This leads to look desperately for new ways of obtaining energy and here is where the renewable energies come in. The energy is always conserved, so the only way of obtaining energy without destroying the Earth is taking it from outside of the planet, and the Sun is a long-term energy emitting source. But this Sun energy (over 1360 W/m^2) [5] is used by nature at countless processes, starting the most important for most of lifeforms on Earth: Photosynthesis.

However, humanity discovered that this energy could be used with the photoelectric effect in order to generate electricity at big scales with the photo-voltaic

cells (PV cells from now on). These use no fuel, only need sunlight to work, being possible to storage it in batteries for nighttime. Using the sunlight directly avoids the waste of energy in other processes, like windmills, which uses something caused by the sun in our atmosphere: the wind.

Despite this, the PV cells are not completely environmentally friendly. There are some issues that make them a environmental hazard, like the land use, the water use during its manufacturing, the chemical products needed to improve the efficiency, etc[6].

There are several materials useful for PV cells construction, changing the efficiency, the cost and the wavelengths they work at. This last, however, can be improved by converting the unused wavelengths into useful ones. The way to do this is by processes of up-conversion and down-conversion.

The spectral conversion is based on transforming a high energy photon and extract 2 photons with less energy (Down-conversion), or the other way around, obtaining one high energy photon from 2 lower energy ones (Up-conversion)[7]. This happens because the rare earth atoms are excited by the photons into a higher energy level, which is unstable, so it decay to the ground state by emitting photon(s) with all the energy excess.

This effect is a hot topic in science and there are many applications to discover for it. Many scientists are working on it as seen in the Shift2017 congress[8], where different applications of the spectral conversion were showed, from energy production (for example, increasing the PV cells efficiency) to medical treatment (cancer cells elimination).

Despite all this, this is not imitating the photosynthesis and, in millions of years of evolution, the plants have chosen this method as their way of obtaining energy, so we can learn from them and obtain Hydrogen as fuel by artificial-photosynthesis. This is based on using the energy held by the H_2 molecule, which is released when it is mixed with oxygen to form water (H_2O). The way of doing this is by obtaining the H_2 with an *artificial leaf*[10] or letting the sun radiation split the water in its components and taking the Hydrogen[11].

The best way to use the sun radiation for water-splitting is in 10 cm depth pools with particles in suspension[11]. This matches with the definition of the traditional canary *salinas*[1]. This is why we are focusing on analyzing the capability of the *salinas* to produce Hydrogen.

---

[1]Salina: pool of few centimeters depth and few square meters area, where the seawater evaporates by the sun impact to obtain salt.

2 Objectives

To produce Hydrogen at the *salinas* is unapproachable yet. So, in this work, we will analyze the viability that the *salinas* have for producing water-splitting by studying the properties of the water and the mud where the water is put on.

In the muds we will be looking for the presence of any type of catalysts. If there were so, the mud would be increasing the efficiency of the process and would be necessary to have it for Hydrogen production.

The water comes directly from the sea and the concentration increases with the water evaporation, so is something to take into account. Besides, to have other substances or organisms that may contribute to the water-splitting is possible, so the measures can differ from what we expect.

Therefore, the point of this work is to set the basis of the research of photocatalysis in the *salinas*' water via analysis of photodegradation of organic dyes dissolved in water.

3 Methodology

3.1 *Salinac*'s Water

A saline is a 10 cm deep pool where you put the seawater in order to let it evaporate for obtaining salt. That place have to meet some requirements so it is efficient enough for salt production. The tradition in the Canary Islands demands to place them on the ground (using a "special mud" that will be explained later), having one or more *cocederos* where the water is partially evaporated so the salt concentration is higher and letting the sun evaporate the water by itself.

Type of water	Arithmetic Mean	Maximum	Minimum
Salinas	7.50	8.30	7.10
Cocedero1	9.05	9.20	7.80
Cocedero2	8.30	8.90	7.70

Table 1: pH of the different types of water which were analyzed

The cycle begins with the first *Cocedero*, more than one meter deep, being filled with seawater. When the level of water have decreased and the salt concentration is higher, the water is moved to the second *cocedero*. Then again, when the level of water is right, it is passed to the *tajos*[2], this time definitively until the water is fully evaporated and there is only salt left. The whole process from filling the *tajos* until the salt is obtained is called a cycle. On the other hand, one full *cocedero* is capable of filling several *tajos*.

All data was taken in the *salinas* of Bocacangrejo in Gran Canaria and following the advises of the *salinas*' worker. These samples were taken with a 100 ml plastic container near to the 20 cm deep in the *cocederos*, while in the tajos the samples were taken with a plastic syringe because of the poor depth, but in both cases we checked that the sample was as clean as possible. In order to measure conductivity, which was needed because there is a well known relation between conductivity and salt concentration, we used a *HACH sension 156*, and for the pH we used a *HI 9811-5* (Figure 1).

In order to obtain a good sampling, we measured the pH and conductivity in some places with different properties: from different parts of both *cocederos*, from different *tajos* at different stages of their cycle. The results showed that there were no significant changes within the same pool, but there were between them (data showed in Table 4). Mainly, what is happening is that the conductivity is increasing, but the pH increases in the first *cocedero* in relation to the sea, which is around 8 [9], and then gets more neutral.

---

[2]*Tajo* is the name of the area where the water is put for salt production

Figure 1: Equipment for measuring conductivity (left) and pH (right)

With these samples, we can compare the efficiency of each salt concentration and see how this influences the water-splitting. Besides, if there is any extra factor contributing to enhance the water-splitting, we can show it by repeating the experiments with *NaCl* dissolved in distilled water at different concentrations.

3.2 Mud Analysis

The owner and the workers of the *salinas* say that the process is efficient due to the "special mud" where they put the water on. This leaded us to analyze the composition of the mud to see which processes are producing a quick disappearance of the water: may it be photocatalysis? If this were so, the mud should contain Titanium (Ti) and/or Iron (Fe) to form Titanium Dioxide (TiO_2), Iron Oxide (Fe_2O_3) or any other photocatalyst.

Scanning Electron Microscopy (SEM) allows us to obtain the proportions between the different elements that a sample is made of and to locate them, becoming able to identify the composition of a specific structure. Although, this tool have problems when the substance is present within the sample in low quantities because the spectral lines, which the software use to identify the elements, are very poor and could be unnoticed due to the background signal.

Figure 2: Photo of B2 and B1 respectively

Thereby we filled two tins with mud, which we called B1 and B2 [3]. In order to introduce them in the SEM, they had to be dried because the water can damage the system. So, we extracted little samples from both B1 and B2, and place them in an absorbent sheet of paper and then into an aluminum container each, in order to introduce both of them in a heater during 24 hours at 30 °C. After that, the samples were taken to the SEGAI (Investigation Management and Support Service) where Juan Luis González Álvarez, the electronic microscopy technician, approved them to be analyzed with the EDXS (Energy Dispersive X-rays Spectroscopy).

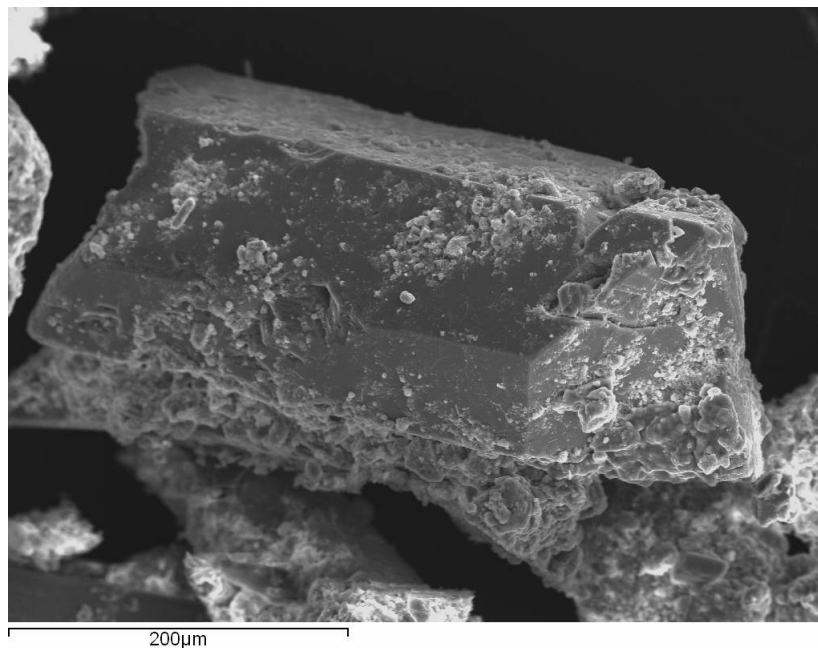
[3]B from *Barro*, which means *mud* in Spanish

Figure 3: Crystal surrounded by an irregular conglomerate (crystal)

First, we took the B2 because it was darker (as seen in the Figure 2) and we thought it could be related to the blackness of the mud. As we had no previous information of the composition, we made a general view of the sample at $Mag^4 = 250$, selecting zones with crystalline shape surrounded by an irregular conglomerate (Figure **??**). Nevertheless, once we analyzed the crystals at $Mag = 1000$, we discovered that they were made of calcium (*Ca*), magnesium (*Mg*) or salt (*NaCl*). No titanium (*Ti*) or iron (*Fe*) were found.

Then we moved to an irregular zone to repeat the process at the same magnifications and we obtained a small amount of *Fe*, but the software did not match the signal with the *Ti* peaks at the spectra. However, we are able to force the system to show where this element would be in the event that it had been present, even if it was not detected in the first place. In this way, a peak can be assigned to the titanium despite the amount is very poor because the peak was clearly distinguished over the background noise as it is shown in the Figure 4.

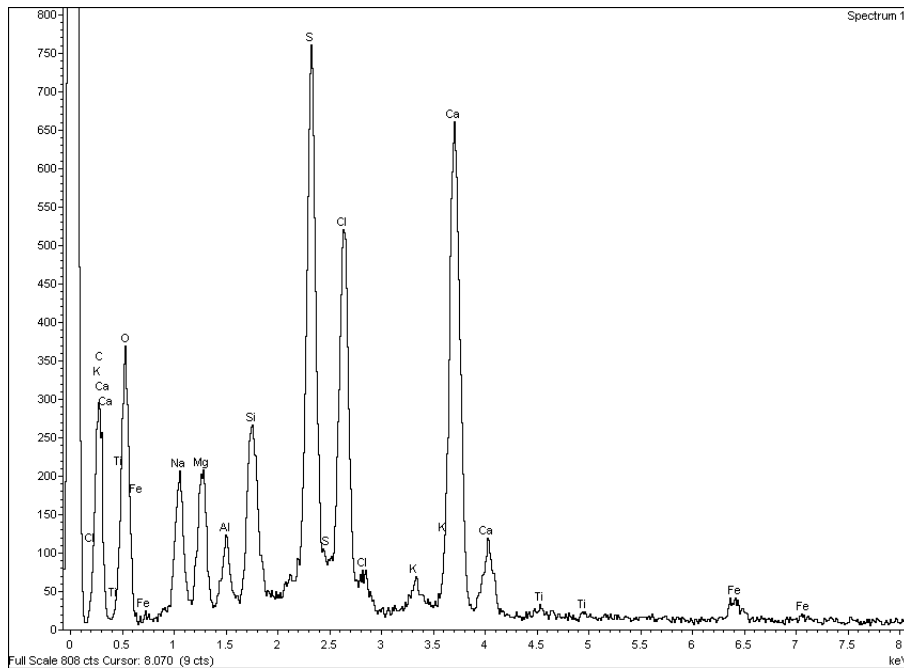[4] *Mag* is refereed to the magnifications

Figure 4: Irregular zone ($Mag = 1000$)

Element	App Conc.	Intensity Corrn.	Weight %	Weight % sigma	Atomic %
O	6.79	0.4365	43.64	1.09	61.26
Na	1.32	0.7046	5.26	0.29	5.14
Mg	0.89	0.6283	3.99	0.22	3.69
Al	0.38	0.7105	1.48	0.14	1.24
Si	1.10	0.8119	3.80	0.19	3.04
S	3.97	0.9171	12.15	0.34	8.51
Cl	2.81	0.7320	10.77	0.33	6.82
K	0.26	0.9719	0.76	0.13	0.44
Ca	5.35	0.9327	16.12	0.41	9.03
Ti	0.09	0.7621	0.34	0.13	0.16
Fe	0.49	0.8193	1.68	0.22	0.68

Table 2: Data from *Irregular zone (Mag = 1000)*

In order to confirm the presence of *Ti* and *Fe*, we selected another irregular area, this time with double the magnifications ($Mag = 2000$) and now the proportions of *Ti* and *Fe* among the other elements were higher (Figure 5), so this time the software identified both of them without forcing it.

Being aware of the presence of these elements, it is possible to locate them with
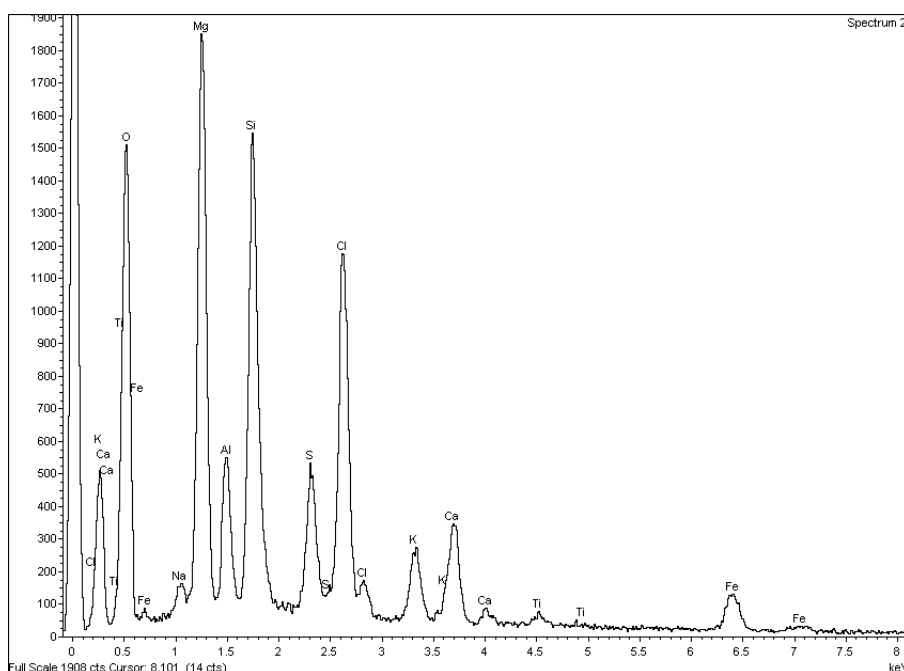
12

Figure 5: Irregular zone ($Mag = 2000$)

a mapping which indicates the point where the signal comes from. This happens by the X-rays diffraction coming from the sample which reach the sensor with different directions and frequencies, being possible to associate each data with a point in the image and with the current chemical elements. So, we can select an element and the software indicates where is it, as it can be seen in the Figure 6. Then we focused in the area where the Ti was concentrated (red spots) and we were able to identify an specific structure once we took the displacement produced by the electron hits into account (the red points would be moved down and to the right). Keeping this in mind, the Ti - Fe object could be the yellow painted one shown in the Figure 7.

Once at $Mag = 6000$ we repeat the analysis of the concentrations and the graph obtained shows a concentration of Ti and Fe (Table 3) almost at the 2% and 1.5%, respectively, of the composition, which is quite high compared with previous results. Despite this, the concentration still low compared with the rest of the constituent elements, being the Magnesium (Mg), the Chlorine (Cl) and the silicon (Si) the most abundant ones, excluding the Oxygen (O) because in the mud it appears combined with other elements forming oxides.

The appearance of strontium (Sr) is remarkable even in little amounts due to its rarity in natural environments, especially if it were present as tausonite (Strontium titanate, $SrTiO_3$), a perovskite structure material (12), not just because it is
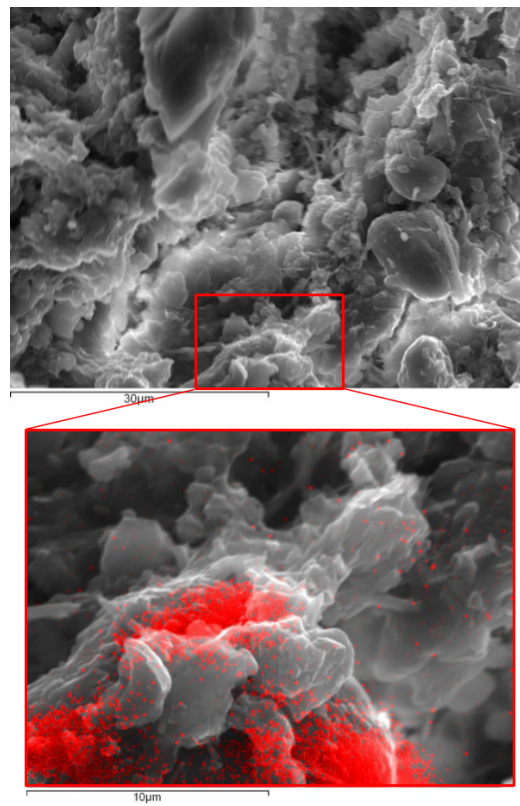
13

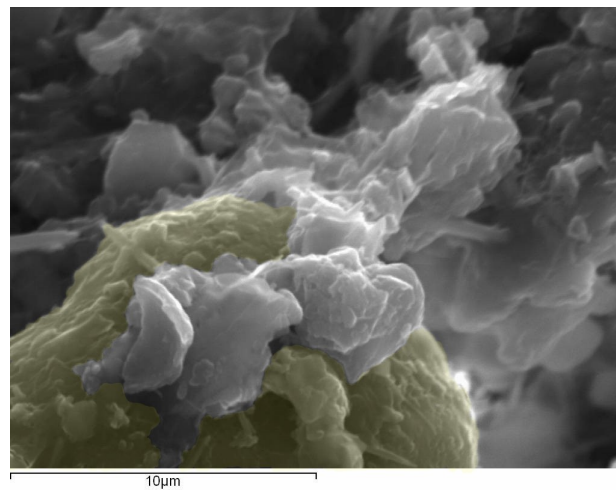Figure 6: Magnification from $Mag = 2000$ to $Mag = 6000$ with the location of the Ti in red

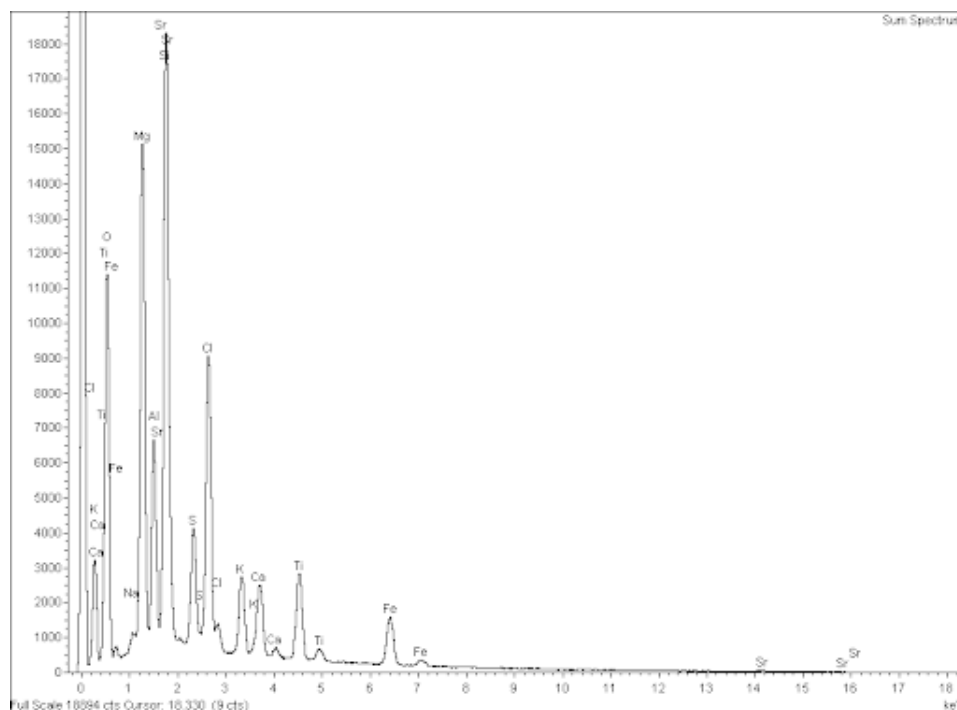Figure 7: Ti and Fe cluster ($Mag = 6000$)

Figure 8: *Ti* and *Fe* cluster (*Mag* = 6000)

Element	App Conc.	Intensity Corrn.	Weight %	Weight % sigma	Atomic %
O	21.81	0.5923	43.78	0.20	60.57
Na	0.33	0.7438	0.52	0.04	0.50
Mg	7.20	0.7119	12.03	0.07	10.95
Al	2.63	0.6824	4.58	0.05	3.76
Si	8.58	0.7488	13.63	0.08	10.74
S	1.91	0.7737	2.94	0.04	2.03
Cl	4.83	0.7024	8.17	0.06	5.10
K	1.86	0.9553	2.32	0.03	1.31
Ca	1.73	0.9267	2.22	0.03	1.23
Ti	2.58	0.8031	3.82	0.04	1.77
Fe	2.60	0.8323	3.72	0.05	1.47
Sr	1.36	0.7148	2.27	0.11	0.57

Table 3: Data from *Irregular zone (Mag* = 6000*)*

unusual, but for its photocatalytic properties, useful for separate the oxygen and hydrogen via water-splitting (13). In our case, the amount of *Sr* is very poor, but it is clearly distinguished over the background noise (Figure 9).
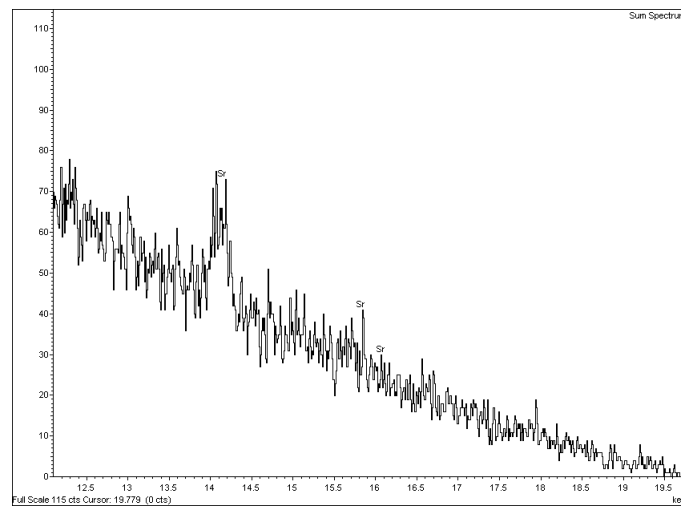
15

Figure 9: *Sr* signal over the background ($Mag = 6000$)

Then, we repeated the procedures with the B1 mud, which means to select an irregular area from only a few magnifications, $Mag = 700$ in this case, and to reveal the concentration of each element. This time the *Fe* and the *Ti* appeared from the very first analysis, and a mapping revealed that both of them were concentrated in some structures, marked in yellow in the Figure 8, but also distributed slightly all over the irregular zones.
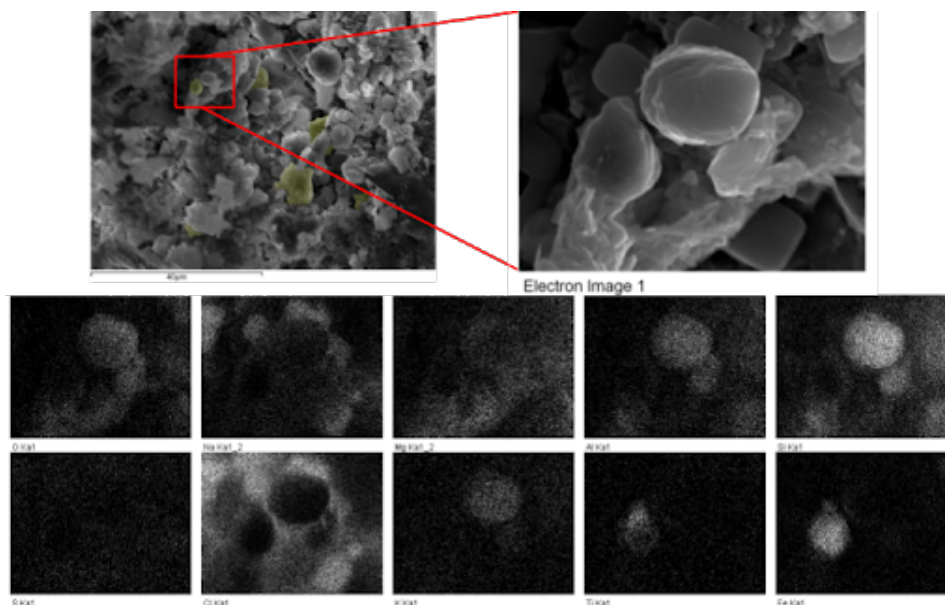

Figure 10: *Ti* and *Fe* cluster (from $Mag = 700$ to $Mag = 10000$)

Focusing on the spherical area at the upper left zone ($Mag = 10000$), we make, again, a deep mapping and the results are shown in the Figure 10. Again, the titanium is located in similar places than the iron. This time the structure is much clearer, but looks no distinct from the adjacent, despite the composition is completely different, so we obtain the same result: sometimes these elements form complex structures but they are not easily distinguished from the others, plus being distributed all over the irregular area. Also the quantity keeps more or less at the same levels, having not too high peaks in the graph.

The last sample we analyzed was another zone of the B1 mud, repeating the same procedures, and in this case the beginning image is at $Mag = 1000$ magnifications and then we amplified to $Mag = 10000$, focusing on a *Fe* and *Ti* bulk that seemed to be a specific structure among the rest of the sample, as the "ball" seen in the Figure 10.

Nevertheless, in this case the cluster seems to be embedded within the surrounding structures, as seen in the Figure 11, but there is no structure difference between the site of interest and the rest of the sample.

Later on, we analyzed the B1 sample again. This time we went straight to an irregular zone and made a mapping hopping to find some signs of *Ti* and *Fe*. The first mapping was at $Mag = 1000$, where we found a few concentrations of both elements; then we increased to $Mag = 3000$ and repeat the procedure, focusing on the main cluster at $Mag = 10000$ (progression shown in Figure 11).

Analyzing the graph at the last position (Figure 12) we discover that around the cluster, there is not as much *NaCl* as in the rest of the sample. There are little changes between the clusters that we have analyzed, and we can see this comparing the graphs of both B1 cluster (Figure 12) and the B2 cluster (Figure 7).
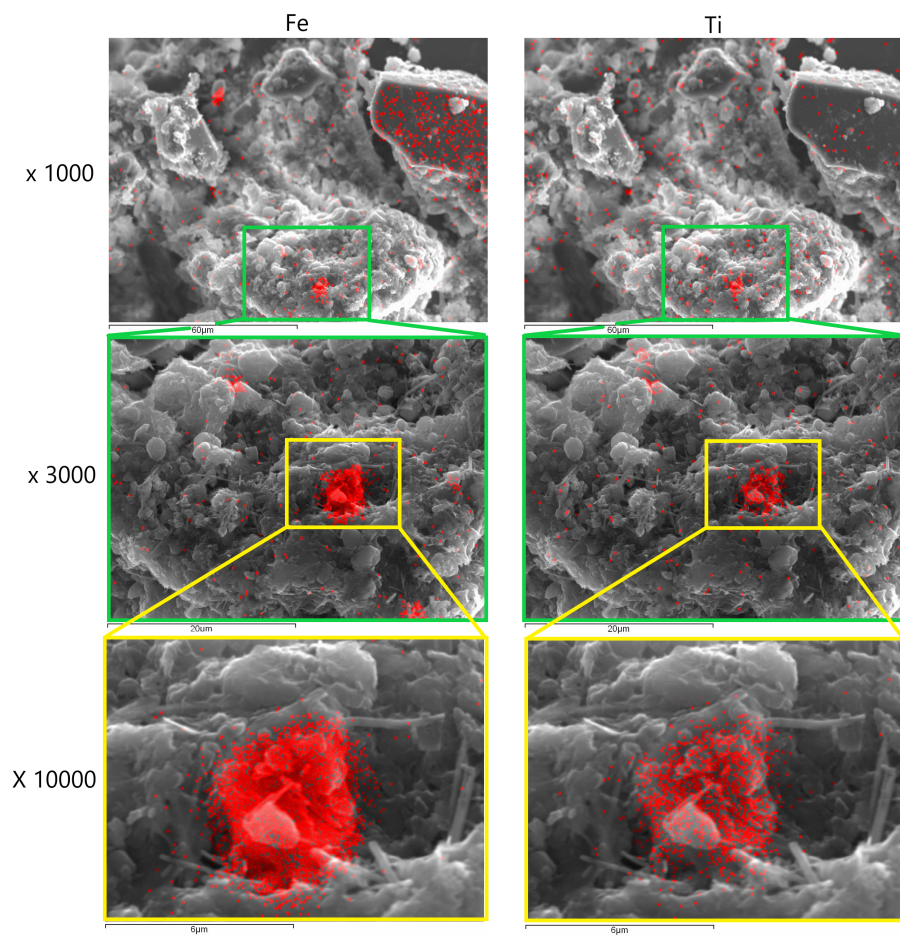
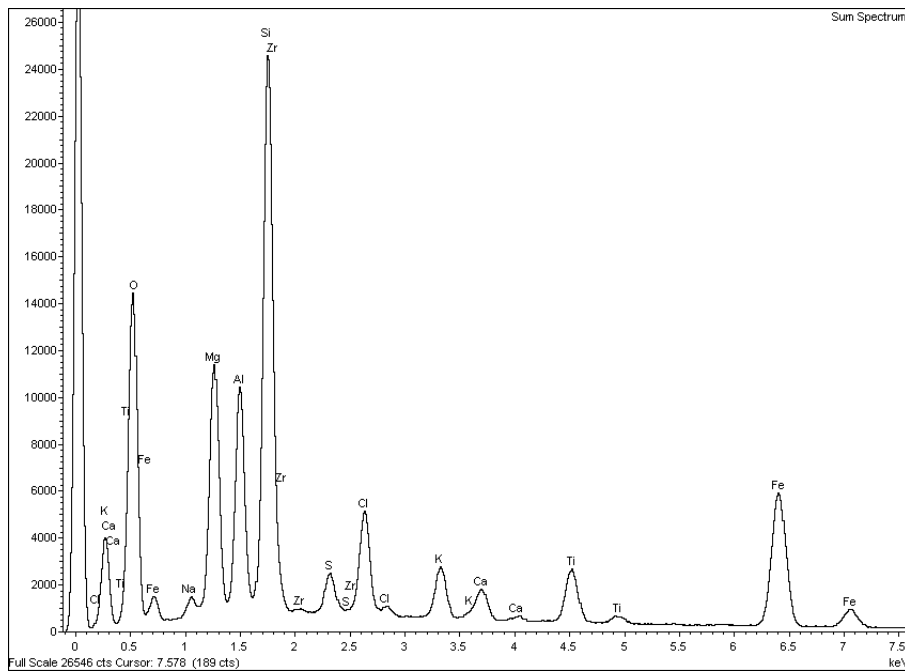Figure 11: Progression of magnifications in the B1 mud

Figure 12: graph of the irregular zone focused on a cluster ($Mag = 10000$)

3.3 Dye Degradation

The final objective is to collect Hydrogen, but working with gases requires complex set ups and the losses are unavoidable. In order to avoid these problems and expenses, we use another system: organic molecules degrade. We have to look for those molecules which react to the presence of H or OH-radicals because this implies the water decomposition in Hydrogen and Oxygen.

For making the photocatalysis we kept the same procedures as we had with distilled water:

1. First, we dilute some dye (the amount depends on the dye) on 100 ml of water, whether distilled or salty. In this point, we have to take the first spectrum with the ultraviolet-visible-infrared (UV-VIS-IR) Perkin-Elmer Lambda 9 spectrophotometer, having a resolution of 0.5 nm and being this spectrum the reference of a unaltered solution.

2. Then, we take a 10 ml sample of the solution and add 4.5 mg of Titanium Dioxide (TiO_2), keeping it at a magnetic agitator with a magnet within the solution. In this moment, the catalyst starts to adsorb a certain percent of the dye.

3. From those 10 ml we extract 2.5 ml with a pipet into a quartz cuvette which is put also on a magnetic agitator. While the rest (7.5 ml) is kept in darkness, the cuvette is lighted from the inside by high energetic up-convertion emission from a $K_2YbF_5 : Tm^{3+}$ crystal with a Tm concentration of 0.2% (the reason that we use this crystal is because it avoids the gap of the TiO_2, as shown in Figure 13[13]), excited with two lasers of 980 nm at 0.66 Watt plus a microscope objective lens ($4\times$) each. To see how well is the crystal emitting, the exceed of light is collected by an optic fiber which sends the signal into a laptop that shows the spectrum of the emitted light.

4. Once the lighting is optimal, the crystal will be up-converting the 980 nm laser light and activating the TiO_2, decomposing the dye. This process happens during an hour.

5. When the process has ended, we centrifuge, at 4000 rpm during 15 minutes, the sample that has been lighted with lasers and the same amount of the solution that has been in darkness. The point of doing this is to precipitate the TiO_2 or any other spot so the the spectrum shows only the contribution of the water and the dye.

6. Finally, we analyze both samples with the spectrophotometer. The one in darkness will show how much does the TiO_2 adsorb, and the one lighted with lasers will show the adsorption plus how much dye has been photocatalyzed. This last will represent the success of the experiment. The decrease
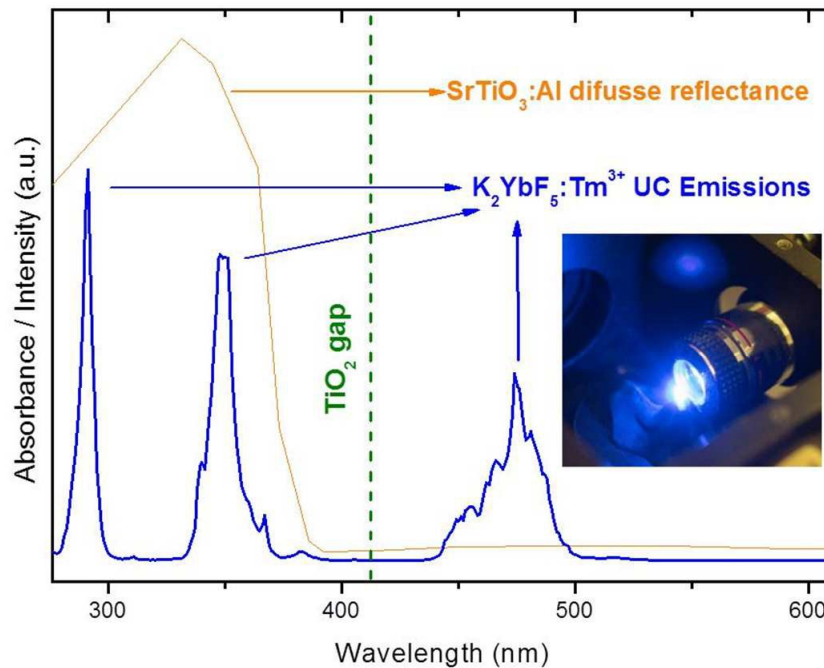
Figure 13: $K_2YbF_5 : Tm^{3+}$ emission avoiding the TiO_2 gap

(or increase) of the absorption is measured from its maximums, around 606 nm and 664 nm.

We take the case of having distilled water as the ideal model, being a situation with known results with most dyes. Then, we repeat the same experiments but with salty water from *salinas* and *cocederos*), with distilled water that we added salt to, and distilled water whose pH is changed, so we can see the reason of the variations at the absorption curves.

3.3.1 Methylene Blue. First approach.

The Methylen Blue (MB) is a blue dye which is used in different industries and is commonly needed to be degraded because it contaminates the water even in little amounts.

With this dye is enough to put 1,0 mg of MB per 100 ml of distilled water [7]. From these solutions will be taken the samples for photocatalysis.

Nevertheless, the first attempt of dissolving the MB in the *salina*'s water was a failure because the water remained transparent. The quantities were not measured
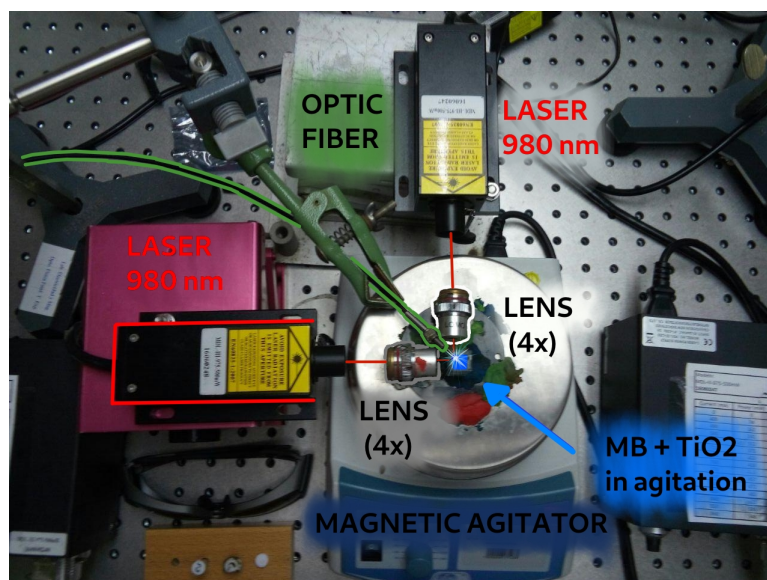
Figure 14: Experimental setup for dye degradation

at first because we just wanted to analyze qualitatively the behaviour of the MB in saline water. We tried to force the solution to dye by adding more MB, but it was useless, the water remained colourless. Then, we mixed it with distilled water at equal proportion and added more MB, which ended up changing the colour.

We suggested three problem sources: the salt, the pH or the plastic of the container where we were making the experiment.

To prove or deny them we started with the material of the container. We added MB to distilled water which was contained in an equivalent plastic container. The dye acted as normal and the spectrum (Figure 15) remained equal during several days, so the plastic had nothing to do with our problem.

In addition to this problem, we had not taken into account that the water in the *salinas* was already saturated of salt, so it could take nothing more. This is why the next experiment is to mix salty water with a solution of MB and distilled water, to avoid the saturation problem and see if the dye disappears. The idea is to dilute 1mg of MB in 10ml of distilled water and then mix this with 90ml of salty water (whether from *cocedero* or *salina*), and this ended up being the most reliable way to proceed that we found.
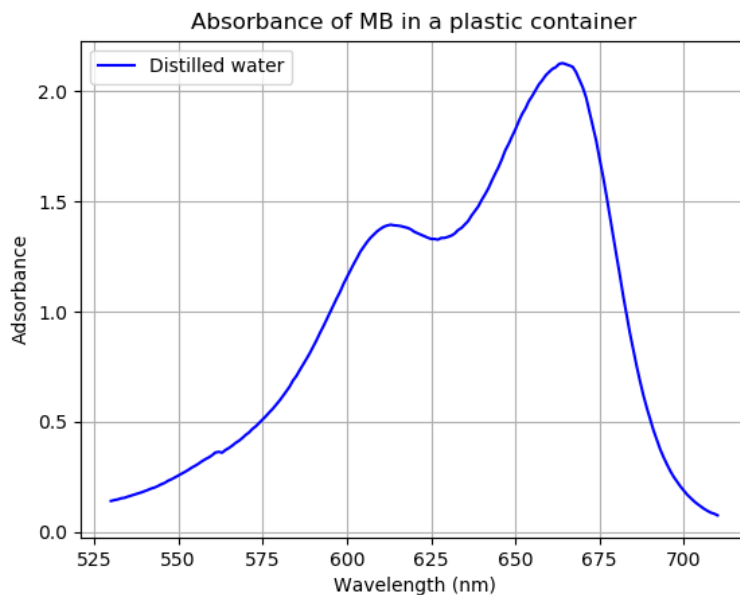
22

Figure 15: Absorbance of the MB in the plastic container

3.3.2 Methylene Blue. Photocatalysis.

The salty water has a specific composition and behaviour, so we have to take into account several things that make the experiment different from its distilled water equal:

1. There is a step in the process where we centrifuge the samples, so it may had an unexpected impact because now the water had particles in suspension, so the absorbance spectrum would be affected-

2. The catalyst could be destroyed by something present in the water that we did not know about.

3. The catalyst could not be well diluted in the liquid because of the saturation caused by the salt.

Due to this, the first step is to analyze the impact of the centrifuge in the solution without having photocatalyzed the dye and then we will be able to give an trustworthy explanation to the results.

3.3.3 Methylene Blue. Salt concentration.

In order to have a good understanding of the salt influence in the process we made 4 samples at different concentrations of salt, one without salt and lineally increase

the amount of salt until the saturation point. Here, we also had to dilute first the MB in distilled water so the process were equal to the previous ones.

The different samples began at 45 ml of distilled water and with 0 g (0% of saturation), 6.5 g (33%), 13.0 g (66%) and 19.5 g (100%) of salt, which is the saturation point for 50 ml of water. The final 5 ml in each sample were added already with the dye, being needed to create a single solution of 20 ml of distilled water with 2.0 mg of MB to distribute among the 4 samples.
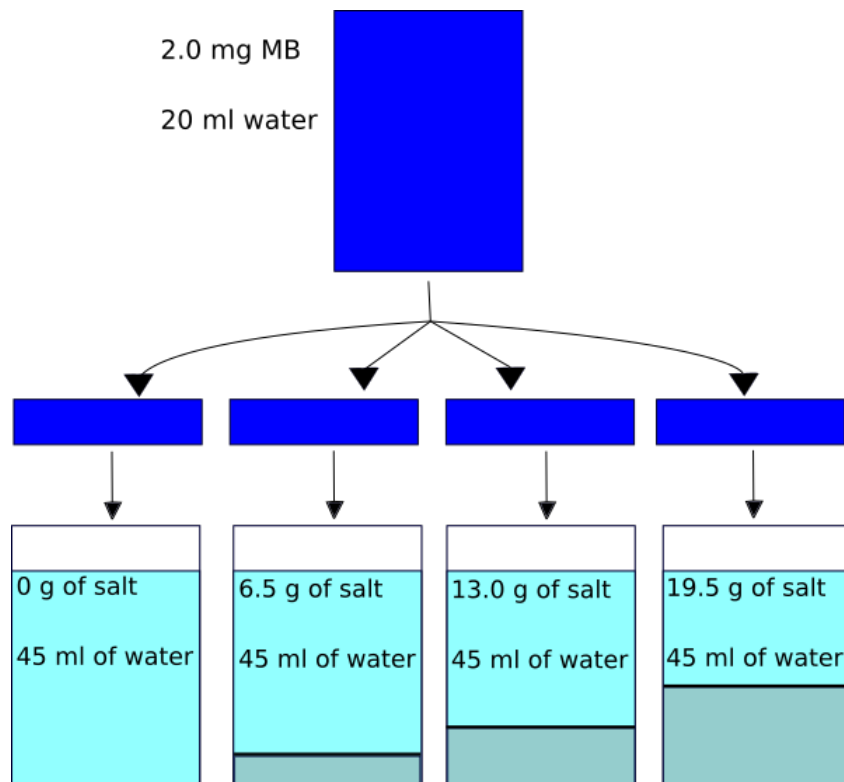

Figure 16: Procedures for the dye distribution

4 Results

4.1 Methylene Blue Degradation

Once the methodology was settled down, we began to make experiments so we could confirm how was the saline water affecting the dye.

First of all, we made a solution of 1 mg of MB within 10 ml of distilled water and then mixed it with 90 ml of *salina*'s water (*Salina1* in the Figure 17)(with 210000 μs of conductivity and 7.4 of pH). We took some spectra at different moments to see how the absorption evolved with time. In addition, we made another solution with *salina*'s water (*Salina2* in Figure 17 and which properties were 222000μs of conductivity and 7.5 of pH) so we knew that the data was actually right. The absorption clearly decreases with time and is possible to see how the colour of the solution is less intense.
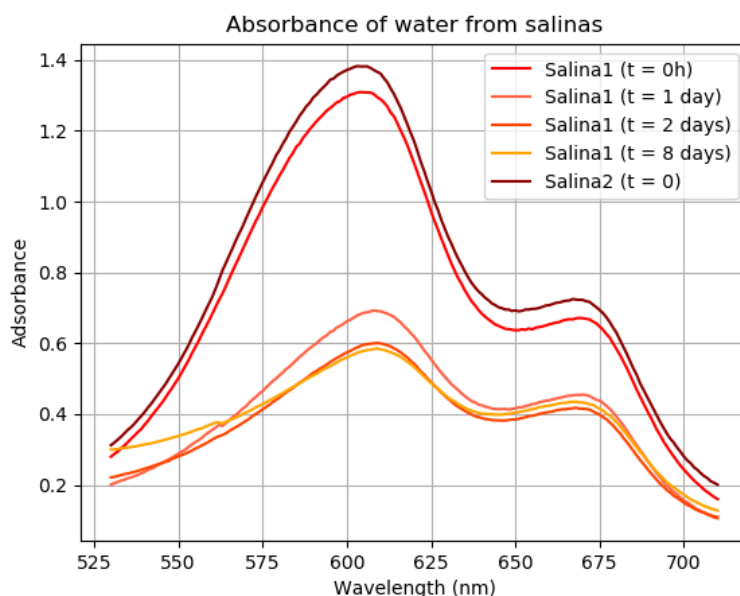

Figure 17: Degradation of the MB without photocatalysis in *salinas*' water

At the same time, we made similar measurements with *cocederos*' water. Again, we made two samples, the first one was made with water from the *cocedero 1* (see Figure 18), which had 64400 μs of conductivity and 9.0 of pH; and in the second one we used the water from the *cocedero 2*, with 96500 μs and a pH of 8.9.

The dye in the *cocedero*'s water stays more or less steady while in the *salina*'s is decomposed and, as the time went by, some kind of purple cloud formed within

25

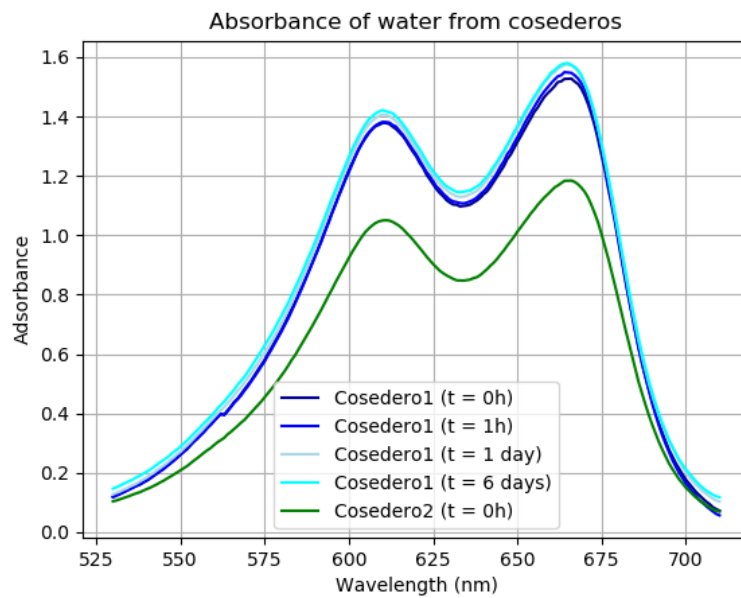Figure 18: Map and table of the *salinas* where the samples where taken

Figure 19: Degradation of the MB without photocatalysis in *cocederos'* water

the water, but this is explained later. This difference led us to establish the *cocedero* as the preferred option for photocatalysis.

4.1.1 Methylene Blue. Photocatalysis.

The first thing to do was to centrifuge[5] some samples so we knew the effect that it produces in the solution. Also we analyzed the adsorption of the TiO_2[6] during half an hour in darkness, so we could know what to expect. This is shown in the Figure 20, where clearly the absorption increases when we centrifuge the sample, which was a surprise because we expected it to drop because of the disappearance of any possible filth present in the seawater. On the other hand, when the adsorption takes place it drops approximately the same quantity that it had increased.
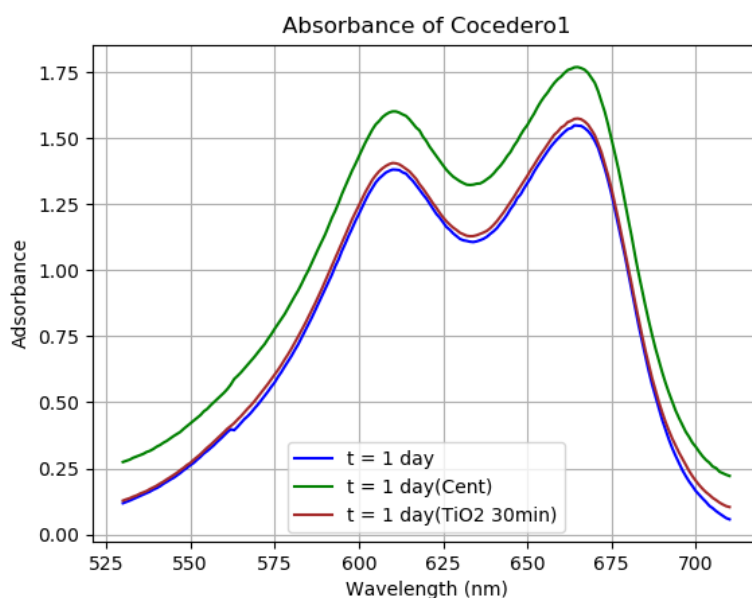

Figure 20: Degradation of the MB without photocatalysis in *cocederos*' water

Once this is made, we began the photocatalysis. Once again the maximums raised in the centrifuged sample and then both of them should decrease, but it only happened in the case of the second photocatalysis (Figure 22), because in the first photocatalysis (Figure 21) only the 664 nm maximum made it, while the 604 nm one increased even a little more. Nevertheless, the change is not significant. In addition, after one hour and a half of being under the action of the $K_2YbF_5 : Tm^{3+}$ producing photocatalysis[7], the absorbance barely dropped in both maximums.

---

[5]"(Cent)" means that the sample has been centrifuged

[6]"(TiO2 X)" means that the sample has been agitated with TiO_2 in darkness during X time, knowing that also implies to be centrifuged
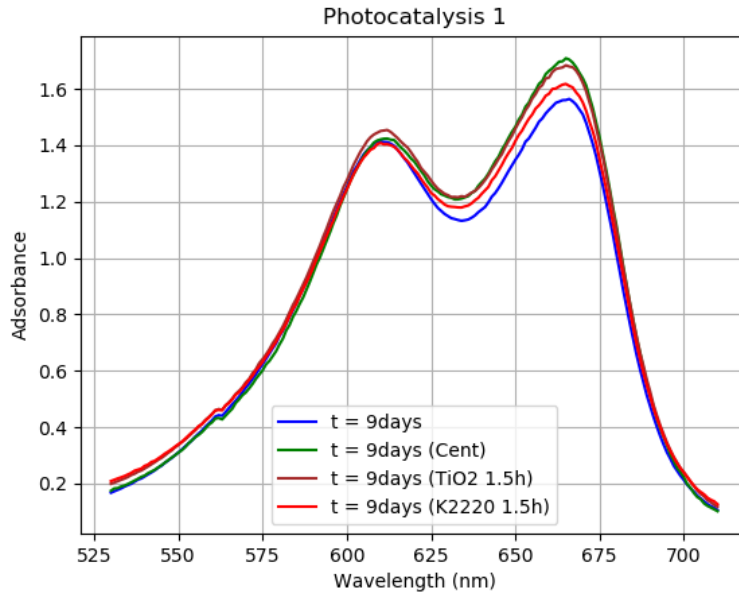
[7]The $K_2YbF_5 : Tm^{3+}$ is referred as K2220

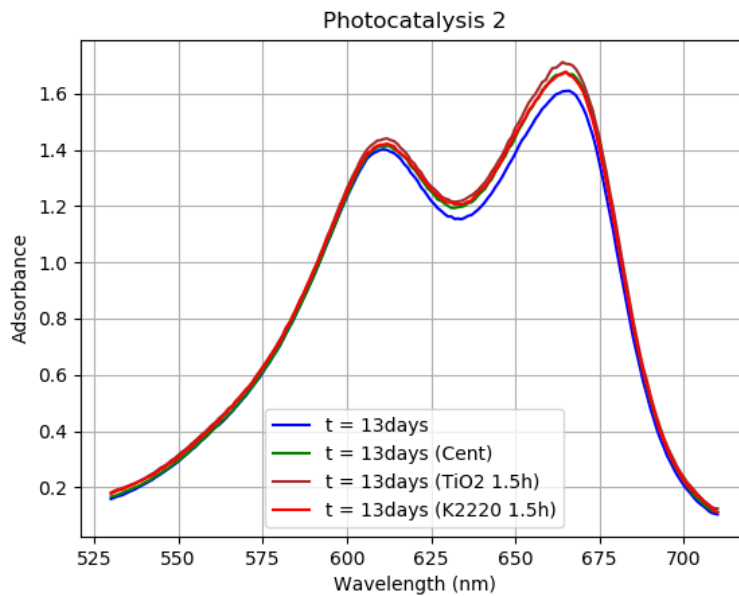Figure 21: Degradation of the MB in photocatalysis in *cocederos*' water

Figure 22: Degradation of the MB in photocatalysis in *cocedero 1*'s water

4.1.2 Methylene Blue. Salt concentration.

When the solutions were made, we took a spectrum from each one at three different times to see the evolution in time of the MB, right after making the mix, the day after and several days later (Figures 23, 24, 25 and 26).
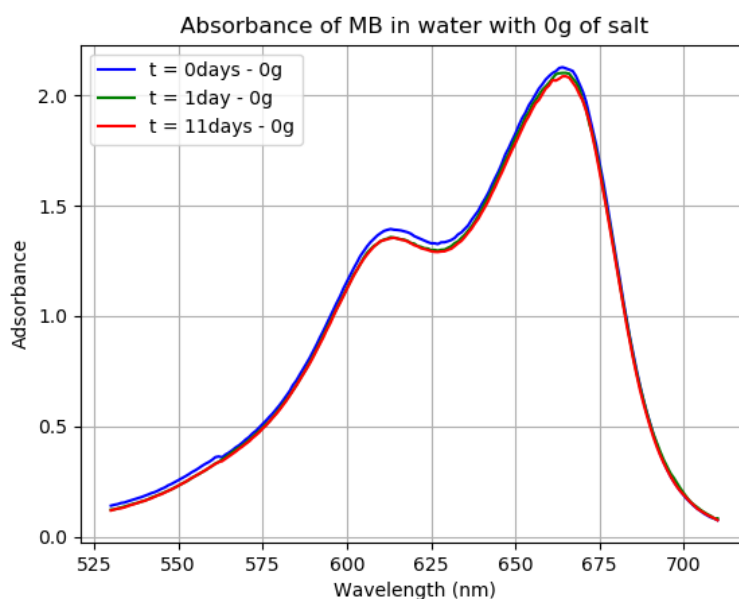

Figure 23: Absorbance of MB at different times with 0g of salt

In this graphics is shown clearly how without the salt the methylene blue is perfectly stable, while the more salt it have, the faster and the more efficiently it decomposes.

Actually we can compare the effects seen at different concentrations with the ones from the *salinas* and the *cocederos* (Figures 27 and 28). Despite the similarities are undeniable, there are also important differences.

The absorbances nearly matches in some points, but none of them follow the exact curve of a *cocedero* or a *salina*. The problem lies in the maximums, which seem to be boosted up in some points and dragged down in others.

If the composition of the samples were the same, this differences would not be so clear, which means that there is something modifying the shape of the absorbance curves that we do not know about.
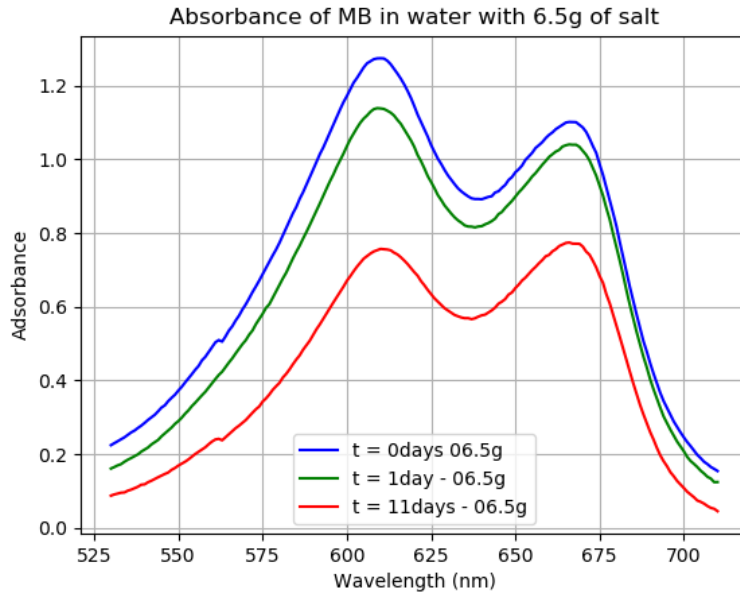
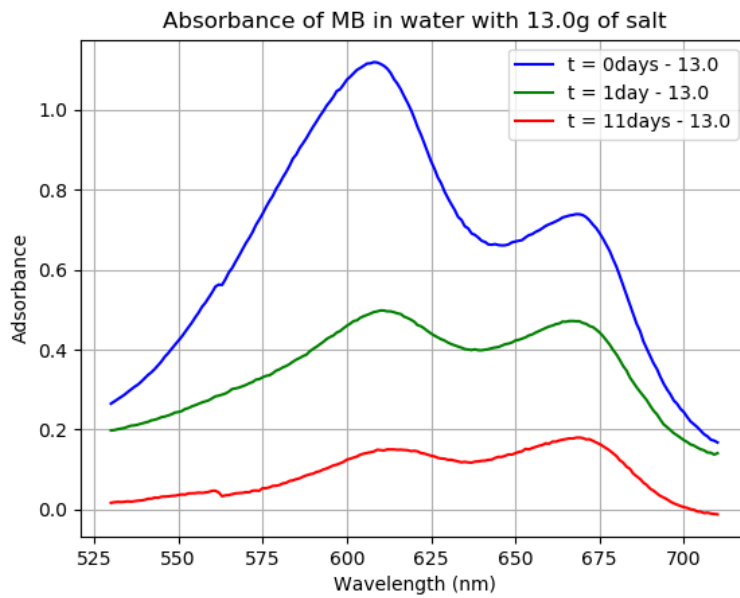Figure 24: Absorbance of MB at different times with 6.5g of salt

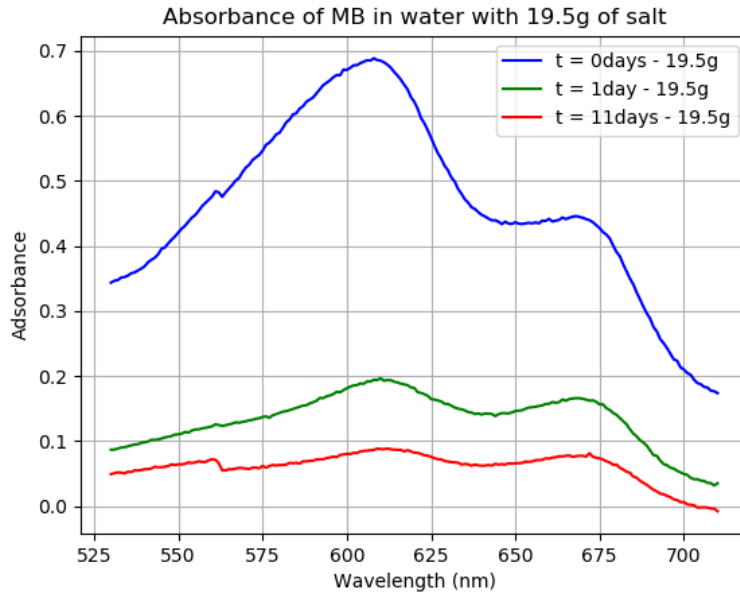Figure 25: Absorbance of MB at different times with 13.0g of salt

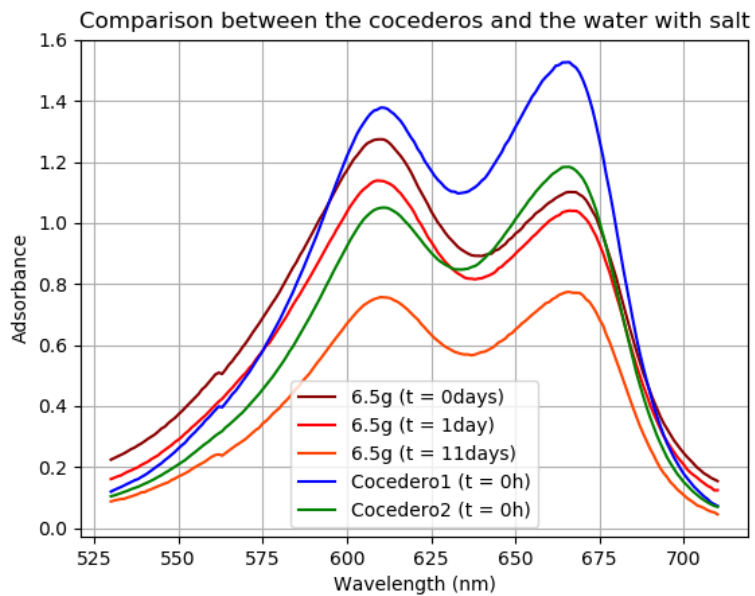Figure 26: Absorbance of MB at different times with 19.5g of salt

Figure 27: Comparison between the Cocedero1 and the water with 6.5g of salt
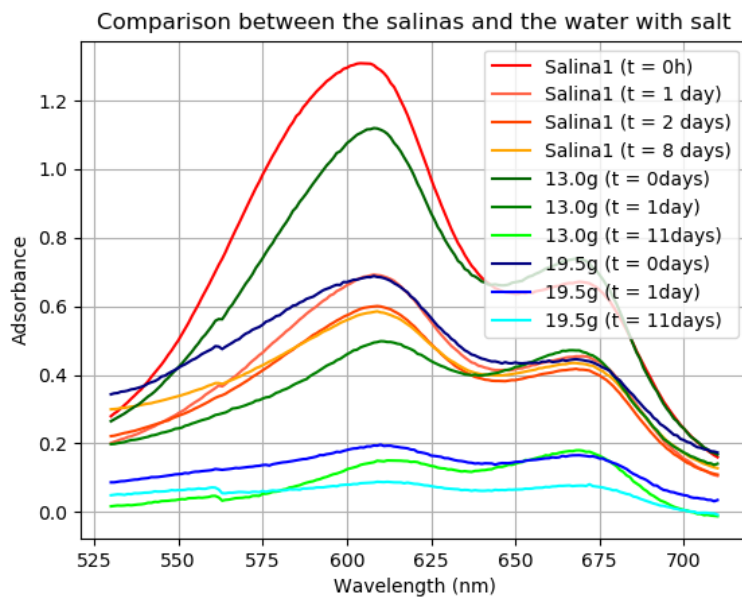
Figure 28: Comparison between the salinas and the water with high concentration of salt

4.1.3 Methylene Blue. Purple Cloud.

Also, with the increase of the salt concentration, the *purple cloud* already mentioned appeared. It did not formed at every solution, but in the most salty ones: on every *salina*, in the one with 13.0 g of salt and in the one with 19.5 g.

Nevertheless, when we took an spectrum of them, the results were totally different, as seen in the Figure 29[8]. The one of the *salina* seems to be more affected by the MB, so we considered the one from the 19.5 g of salt solution, the one to analyze.
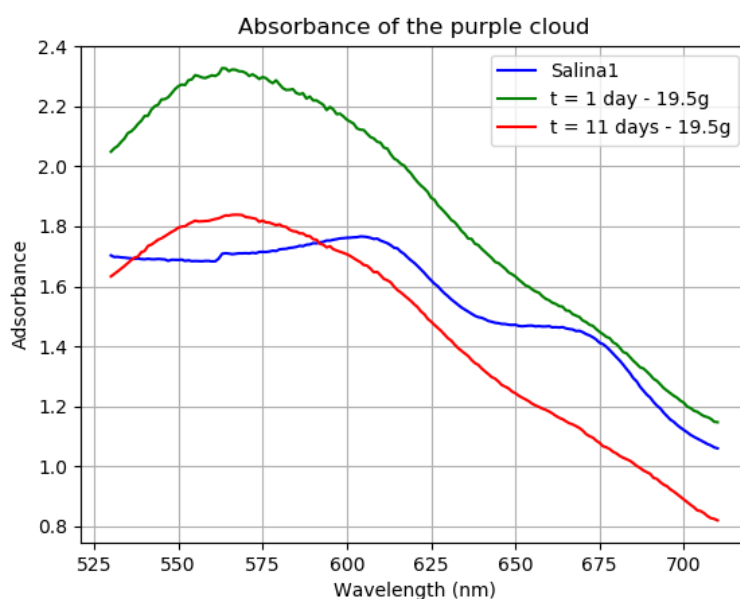
Figure 29: Comparison between the salinas and the water with high concentration of salt

In any case, the spectra seems to be uncompleted, so we took a full range spectrum of the *purple cloud* and another from the decomposed MB of the same sample (the one with 19 g of salt) (Figure 30).

The MB is almost decomposed and the maximums at 606 nm and 664 nm are almost gone, but they still take place in both spectra.

---

[8]There is no spectrum of the solution with 13 g of salt because there was not enough *purple cloud* for doing it.
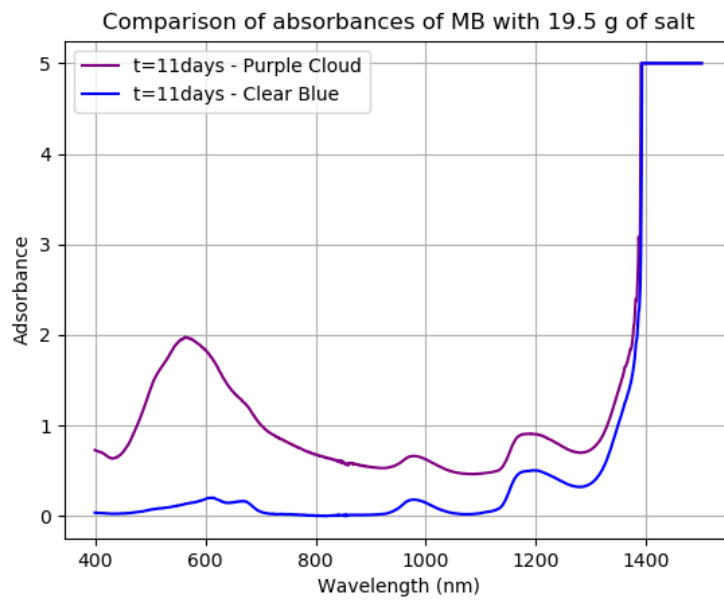
Figure 30: Comparison between the salinas and the water with high concentration
of salt

5 Conclusions

At the beginning, the idea was to make huge improvements with the *salinas'* water, as shown in the following video, which ULL-Media made with us for divulgation purposes: `https://www.youtube.com/watch?v=cvZuLGF7VM4&feature=youtu.be`.

Nevertheless, during this work there has been several issues that complicated the improvement. Even so, there are some useful conclusions.

1. The mud have so little amounts of *Fe* and *Ti* that is not possible to prove the presence of photocatalysts within them. But, those elements are there and may have little contribution to the water evaporation in the *salinas*. If not, there have to be something else that make the *salinas'* workers call it "special mud".

2. The methylene blue is clearly not working with the salt, so it have to be changed for another dye that resists it. After weeks of search, we discovered that the Reactive Black 5 could be an option(**?**). This dye is also affected by the salt, but it resists with intense absorbance spectra. In addition, reacts with the TiO_2, so there is little to change in the experimental setup.

3. The water from the *salinas* contains more things than just salt and we do not know what yet. However, these could be helping or complicating the photocatalysis without our consciousness.

The results are different from what we expected, but another step is settled in the search for the clean energy.

6 Bibliography

References

[1] Carbon Dioxide Information Analysis Centre
https://cdiac.ess-dive.lbl.gov/trends/co2/lawdome.html

[2] Carbon Dioxide Information Analysis Centre
https://cdiac.ess-dive.lbl.gov/pns/current_ghg.html

[3] Banco Mundial de Datos
https://datos.bancomundial.org

[4] European Database
https://ec.europa.eu/eurostat/data/database

[5] Greg Kopp; and Judith L. Lean. GEOPHYSICAL RESEARCH LETTERS, VOL. 38, L01706, **2011**

[6] Union of Concerned Scientist
https://www.ucsusa.org/clean_energy/our-energy-choices/
renewable-energy/environmental-impacts-solar-power.html

[7] Lothar Wondraczek; Esa Tyystjärvi; Jorge Méndez-Ramos; Frank A. Müller; and Qinyuan Zhang. Adv. Sci. **2015**, 1500218

[8] Shift 2017 congress
http://www.shift2017.es/

[9] G.M. Marion, F.J. Millero, M.F. Camões, P. Spitzer, R. Feistel, C.-T.A. Chen. Marine Chemistry 126 (2011) 89–96

[10] D. Nocera. ACCOUNTS OF CHEMICAL RESEARCH, 767–776, **2012**, Vol. 45, No. 5

[11] Blaise A. Pinaud, Jesse D. Benck, Linsey C. Seitz, Arnold J. Forman, Zhebo Chen, Todd G. Deutsch, Brian D. James, Kevin N. Baum, George N. Baum, Shane Ardo, Heli Wang, Eric Miller and Thomas F. Jaramillo. Energy Environ. Sci., 2013, 6, 1983

[12] Je-Deok K IM; Toshiyuki M ORI; and Itaru H ONMA. Japanese Journal of Applied Physics, Vol. 46, No. 19, **2007**, pp. L 468– L 470

[13] David M. Fabian; Shu Hu; Nirala Singh; Frances A. Houle; Takashi Hisatomi; Kazunari Domen; Frank E. Osterloh; and Shane Ardo. Energy Environ. Sci., **2015**, 8, 2825

7 Appendix

These are measures taken in December 2017 and it rained several days, so the characteristics of the water changed[9].

Row/Column	Date	pH	Temperature (^{o}C)	Conductivity ($\mu s/cm$)
F05 C03	15/12/2017	7.5	19.9	235000
F05 C03	16/12/2017	7.5	23.5	234000
F05 C03	21/12/2017	N	N	N
F05 C03	23/12/2017	N	N	N
F05 C03	26/12/2017	N	N	N
F05 C03	28/12/2017	N	N	N
F05 C03	29/12/2017	8.2	19.9	121900
F11 C01	15/12/2017	7.5	21.0	213000
F11 C01	16/12/2017	7.4	24.6	211000
F11 C01	21/12/2017	7.4	25.7	214000
F11 C01	22/12/2017	7.4	21.9	210000
F11 C01	23/12/2017	7.3	24.2	205000
F11 C01	26/12/2017	7.2	21.9	125100
F11 C01	28/12/2017	7.1	25.6	197200
F11 C01	29/12/2017	7.8	19.8	223000
F15 C03	15/12/2017	7.6	20.5	227000
F15 C03	16/12/2017	7.5	24.6	227000
F15 C03	21/12/2017	7.4	25.2	229000
F15 C03	22/12/2017	7.5	23.4	215000
F15 C03	23/12/2017	7.4	23.7	215000
F15 C03	26/12/2017	7.6	21.8	175500
F15 C03	28/12/2017	N	N	N
F15 C03	29/12/2017	8.3	18.4	69000
F17 C01	18/12/2017	7.6	24.6	221000
F17 C01	19/12/2017	7.7	20.4	230000
F17 C01	20/12/2017	7.5	20.0	226000
F17 C01	21/12/2017	7.5	28.2	225000
F17 C01	22/12/2017	7.5	22.2	216000
F17 C01	23/12/2017	7.4	22.8	218000
F17 C01	26/12/2017	7.5	22.0	194300
F17 C01	28/12/2017	N	N	N
F17 C01	29/12/2017	N	N	N

---

[9]The "N" means that there is no data, whether because there was no water left in the tajo, or because of a human error

Row/Column	Date	pH	Temperature (ºC)	Conductivity (µs/cm)
F21 C08	15/12/2017	7.5	22.4	232000
F21 C08	16/12/2017	7.4	21.8	232000
F21 C08	19/12/2017	7.5	20.4	234000
F21 C08	20/12/2017	7.5	19.6	N
F21 C08	21/12/2017	7.4	22.6	210000
F21 C08	22/12/2017	7.4	24.6	231000
F21 C08	23/12/2017	7.3	24.9	228000
F21 C08	26/12/2017	7.4	22.3	204000
F21 C08	28/12/2017	N	N	N
F21 C08	29/12/2017	8.3	18.4	72400
F22 C03	15/12/2017	7.5	22.8	227000
F22 C03	16/12/2017	7.4	24.2	221000
F22 C03	21/12/2017	7.5	24.3	222000
F22 C03	22/12/2017	7.5	24.5	222000
F22 C03	23/12/2017	7.4	24.5	215000
F22 C03	26/12/2017	7.3	22.3	181300
F22 C03	28/12/2017	7.2	23.3	185400
F22 C03	29/12/2017	8.2	19.0	79400
F29 C04	15/12/2017	7.8	21.2	229000
F29 C04	16/12/2017	7.7	24.0	228000
F29 C04	19/12/2017	7.9	21.2	233000
F29 C04	20/12/2017	7.8	20.7	231000
F29 C04	21/12/2017	7.7	23.9	232000
F29 C04	22/12/2017	7.7	23.4	228000
F29 C04	23/12/2017	7.5	24.5	223000
F29 C04	26/12/2017	7.5	21.7	219000
F29 C04	28/12/2017	7.5	22.9	215000
F29 C04	29/12/2017	N	N	N
Cosedero 1	15/12/2017	9.2	19.5	63600
Cosedero 1	16/12/2017	8.8	19.6	63400
Cosedero 1	18/12/2017	8.9	20.0	63100
Cosedero 1	19/12/2017	9.1	21.5	64100
Cosedero 1	20/12/2017	9.1	21.2	64100
Cosedero 1	21/12/2017	9.0	21.5	64400
Cosedero 1	22/12/2017	9.1	20.7	65000
Cosedero 1	23/12/2017	N	N	N
Cosedero 1	26/12/2017	9.1	20.7	66200
Cosedero 1	28/12/2017	7.8	20.3	60300
Cosedero 1	29/12/2017	8.3	18.8	63800

Row/Column	Date	pH	Temperature (°C)	Conductivity (μs/cm)
Cosedero 2	15/12/2017	8.7	18.9	93300
Cosedero 2	16/12/2017	8.2	19.5	92700
Cosedero 2	18/12/2017	8.2	18.8	91800
Cosedero 2	19/12/2017	8.7	18.5	N
Cosedero 2	20/12/2017	8.5	18.1	95400
Cosedero 2	21/12/2017	8.9	18.5	96500
Cosedero 2	22/12/2017	8.8	18.8	97500
Cosedero 2	23/12/2017	8.3	18.2	97900
Cosedero 2	26/12/2017	8.2	17.4	102100
Cosedero 2	28/12/2017	7.7	19.7	65200
Cosedero 2	29/12/2017	8.0	18.8	63400

Table 4: All data from the different types of water which were analyzed

Figure 31: Spectrophotometer used to measure absorbances

Figure 32: Gradient of salt concentration from 0g (left) to 19.5g(right)

Figure 33: Purple cloud in two different samples